

THE INFLUENCE OF ENVIRONMENT ON THE STAR FORMATION RATES OF GALAXIES

Yasuhiro Hashimoto and Augustus Oemler, Jr.

Carnegie Observatories, 813 Santa Barbara St., Pasadena, CA 91101 USA; and
Department of Astronomy, Yale University, P.O. Box 208101, New Haven, CT 06520-8101
USA; hashimot@astro.yale.edu, oemler@ociw.edu

Huan Lin

Department of Astronomy, University of Toronto, Toronto, Ontario, M5S 3H8, Canada;
lin@astro.utoronto.ca

and

Douglas L. Tucker

Fermilab, MS 127, PO Box 500, Batavia, IL 60510 USA; dtucker@fnal.gov

ABSTRACT

We have used a sample of 15749 galaxies taken from the Las Campanas Redshift Survey (Shectman et al. 1996) to investigate the effects of environment on the rate of star formation in galaxies. For each galaxy we derive a measure of star formation rate (SFR) based on the strength of the [OII] emission line, and a measure of galactic structure based on the central concentration of the galaxy light, which is used to decouple the effect of “morphology-environment” relation from the SFR. Galactic environment is characterized *both* by the three-space local density of galaxies and by membership in groups and clusters.

The size and homogeneity of this data set allows us to sample, for the first time, the entire range of galactic environment, from the lowest density voids to the richest clusters, in a uniform manner. Thus, we could expand our research from the conventional cluster vs. field comparison to a new “general” environmental investigation by decoupling the local galaxy density from the membership in associations. This decoupling is very crucial for constraining the physical processes responsible for the observed environmental dependencies of star formation. On the other hand, the use of an automatic measure of galactic structure (concentration index), rather than Hubble type which is subjective and star formation-contaminated estimate of galactic morphologies, allows us to cleanly separate the morphological component from the SFR vs. environment relationship.

We find that, when cluster/field comparison is made, cluster galaxies exhibit *reduced* star formation *for the same concentration index*. This result supports several previous Hubble type-based studies reporting similar suppressions of star formation among cluster galaxies for the same Hubble type. We did not find any qualitatively different responses to environments between early and late type spirals, which were also previously reported. On the other hand, a further division of clusters by “richness” reveals a new possible excitation of starbursts in groups and poor clusters.

Meanwhile, a more general environmental investigation shows that the star formation rate of galaxies of a given concentration index is sensitive to local galaxy density and shows a continuous correlation with the local density, in such a way that galaxies show higher levels of star formation in low density than in high density environments. Interestingly, this trend is also observed both inside and outside of clusters, implying that physical processes responsible for this correlation might not operate intrinsically in the cluster environment. Furthermore, a more complex facet of the dependence of SFR on local density is also revealed; galaxies with differing levels of star formation appear to respond differently to the local density. Low levels of star formation, corresponding to those expected in normal members of the Hubble sequence, are more sensitive to environment inside than outside of clusters. In contrast, high levels of star formation, identified as “starbursts”, are at least as sensitive to local density in the field as in clusters.

We conclude that at least two separate processes are responsible for the environmental sensitivity of the SFR, and tentatively identify gas removal processes as responsible for the variation with density of the SFR of normal galaxies, and galaxy-galaxy interactions as responsible for the prevalence of starbursts in intermediate density environments.

Subject headings: galaxies:clusters:general — galaxies:evolution — galaxies:interactions — galaxies:starburst — galaxies:stellar content — galaxies:structure

1. INTRODUCTION

Many lines of evidence, accumulated over the past several decades, have made it abundantly clear that there has been substantial evolution of the properties and populations

of galaxies during recent epochs ($z \leq 1.0$). Such evolution is seen both in clusters (Butcher & Oemler 1984; Dressler et al. 1994), in groups (Allington-Smith et al. 1993) and in the general “field” population (Lilly et al. 1996, Glazebrook et al. 1995). Although it is possible that some portion of the evolutionary changes observed are due to causes internal to the individual galaxies, there are reasons for suspecting that much of the evolution is driven by external forces in the galaxies’ environment.

Firstly, there is some evidence which suggests that the rate at which galaxies of a given type have evolved varies substantially with environment (Allington-Smith et al. 1993). Secondly, the profound changes in the global properties of galaxies which have occurred during recent epochs are difficult to understand using only the processes occurring within an undisturbed, isolated galaxy. Finally, the large systematic variations in galaxy populations with environment *require* that environment affected the properties of galaxies no earlier than the epoch of their formation.

A number of modes of interaction of galaxies and their surroundings are known which can be expected to cause significant changes in the properties of galaxies over time, and at least some examples of such processes in action have been discovered in low and intermediate redshift galaxy populations. Among these processes are galaxy-galaxy mergers (e.g. Barnes & Hernquist 1991), tidal interactions between galaxies and surrounding masses (e.g. Byrd & Valtonen 1990), and gas-phase interactions between the intragalactic and intergalactic media (e.g. Gunn & Gott 1972; van den Bergh 1976; Dressler & Gunn 1983). Unfortunately, however easily one may enumerate processes to drive galaxy evolution, and however plausible such mechanisms may be, there exists little evidence demonstrating that any one of these processes is, in fact, responsible for driving galaxy evolution. Most of these processes act over an extended period of time, while observations of any population of galaxies give one only a snapshot of one instant in its history. Also, observations at intermediate and high redshifts, which have provided most of the evidence for galaxy evolution, cannot easily provide the detailed information which is needed to elucidate subtle and complicated processes.

However, any means by which galaxies interact with their surroundings should operate today as well as at earlier times, and, therefore, observations of nearby populations should be an effective way of understanding them. In addition to direct evidence for the occurrence of interactions capable of driving galaxy evolution, the local universe holds clues about the nature of those phenomena in the form of variations of galaxy properties with environment, which must be the result of past interactions. The most well-established of such variation is the morphology-density relation (Dressler 1980), which appears to hold not only in clusters, but also in the field (Bhavsar 1981; de Souza et al. 1982; Postman & Geller 1984; Giovanelli

& Haynes 1986; Tully 1988). However, another, perhaps equally important clue for the understanding of the origin and the evolution of galaxies can be obtained by the study of the influence of environment on star formation of galaxies, since star formation is both a fundamental galactic parameter and a driver of galaxy evolution.

There have been many studies investigating environmental influences on star formation. However, these previous studies have been limited to cluster vs. field comparisons (or similar membership comparisons) which compare star formation in cluster galaxies to that in a field control sample. Unfortunately, these studies have produced conflicting results. Some have suggested a *reduced* star formation rate (SFR) in cluster galaxies with respect to field galaxies of the same morphological type (e.g., Gisler 1978; Kennicutt 1983; Dressler, Thompson & Sheckman 1985). However, other studies suggest a similar or *higher* SFR in cluster spirals with respect to the field sample (e.g., Kennicutt et al. 1984; Gavazzi & Jaffe 1985). Others report qualitatively differential responses to environment between early and late type galaxies (e.g. Moss & Whittle 1993).

Some of the inconsistency between previous cluster/field studies can be traced to two facts. Firstly, these studies use small samples for both cluster and field subsets (at most, on the order of 10^2 galaxies in each subset). With samples of this size it is difficult to make a statistically sound comparison, particularly after binning galaxies by Hubble type. Also, the field samples are usually selected from existing bright galaxy catalogs, or from “pencil beam” studies, which, despite a careful effort to select a fairly normal cross section of galaxies, may contain galaxies from a wide variety of environments. Thus “field” samples may contain galaxies within loose groups or the periphery of clusters which dilute the contrast with the cluster samples. Secondly, most of the previous cluster/field studies were forced to combine multiple data sets with heterogeneous characteristics, such as different Hubble classifications by different observers, varying image quality, different star formation measures with different sensitivity, and even different selection criteria of sample objects, all of which can cause spurious results.

It is clear that a new cluster/field comparison using a large number of galaxies studied in a consistent manner is very much needed. However, even a cluster vs field comparison free of these problems is not sufficient. The cluster/field studies (or any studies comparing subsets which are selected on the basis of membership in galaxy associations) have a fundamental limitation for understanding the mechanisms responsible for the environmental influences on star formation. In such studies, the inability to decouple very local environment, as characterized, for example, by local galaxy density, from more global environments, such as membership in a cluster, prevents us from differentiating between mechanisms specific to each of these classes of environment. The significance of the

distinction between local and broader environments has been a matter of much contention in cluster studies (see, for example, Dressler 1980 vs. Whitmore & Gilmore 1991)

A further, equally serious, problem with previous studies comes from the nature of the Hubble type itself, which has been used for the normalization of star formation rates over the broad range of galaxy types. The Hubble type is determined by multiple characteristics of a galaxy, one being the resolution of spiral arms. However, the resolution of spiral arms is, in practice, determined largely by the star formation activity in the arms. Thus, systematic variations in the star formation may cause a systematic shift in the Hubble type. When Hubble type is used to normalize star formation rates, this shift results in a serious reduction in the sensitivity of the measurement of varying star formation rates. To avoid this, we need to characterize the galaxies not by Hubble type, but rather by a physical parameter which is more independent of star formation. (The problem of the Hubble system is further discussed in §5.)

In this paper, we present our first attempt to answer questions about general environmental effects on the star-forming properties of galaxies in the local universe, taking advantage of the very large and homogeneous data set available from the Las Campanas Redshift Survey (LCRS; Shectman et al. 1996). This data set consists of a large number of galaxies inhabiting the entire range of galactic environments, from the sparsest field to the densest clusters, thus allowing us to study environmental variations without combing multiple data sets with inhomogeneous characteristics. Furthermore, we can also extend our research from the traditional cluster/field comparison to more “general” environmental study by, for the first time in investigations of star formation properties, decoupling the local galaxy density from the membership in associations. Finally, to minimize the problems with the use of Hubble types mentioned above, we have used an automatically measured concentration index as a star formation baseline.

The outline of this paper is as follows. §2 briefly describes the dataset used. In §3 we describe the spectroscopic measures of star formation, and in §4 we discuss the method of analysis. Results are in §5.

2. DATA

Here we briefly describe our survey parameters; the reader is referred to Shectman et al. (1996) for further details. The LCRS consists of 26418 galaxies, with a mean redshift $z = 0.1$, and a depth of about $z = 0.2$. The survey galaxies were selected, using isophotal and central magnitude criteria, from CCD-based photometry in a “hybrid” Kron-Cousin

R band. This photometry was obtained from driftscans on the Las Campanas 1m Swope Telescope. The survey covers over 700 square degrees in six $1.5^\circ \times 80^\circ$ “slices” in the North and South galactic caps. Every slice consists of over 50 $1.5^\circ \times 1.5^\circ$ spectroscopic fields, each containing a maximum of 50 or 112 galaxies. The first 20% of the redshifts were obtained using a 50-object fiber-optic spectrograph. The nominal isophotal magnitude limits of the spectroscopic sample were $16.0 \leq R \leq 17.3$, and an additional central magnitude limit excluded the 20% of galaxies of lowest central surface brightness. The rest of the redshifts were obtained with a 112-object fiber system, with isophotal limits of $15.0 \leq R \leq 17.7$, and exclusion of the 5-10% of galaxies with lowest central surface brightness. The shape of the luminosity function of the LCRS is consistent with that of other redshift surveys (Lin et al. 1996).

The spectra were obtained with the multi-fiber spectrograph and Reticon detector mounted on the du Pont 2.5m telescope at Las Campanas Observatory. Each spectrum was flat fielded, wavelength calibrated, and sky subtracted. The spectra have a wavelength range of 3350-6750 Å, with a resolution of ~ 5 Å and a pixel scale of ~ 3 Å. The average signal-to-noise in the continuum around the Balmer absorption lines is 8 to 9.

3. SPECTROSCOPIC MEASURES

In order to quantify the star formation properties of LCRS galaxies, we have measured the equivalent width (EW) of [OII] λ 3727, [OIII] λ 5007, and $H\beta$ in LCRS spectra. Conventionally, $H\alpha$ has proved to be the best optical indicator of the massive star formation rate (e.g. Kennicutt 1983). However, $H\alpha$ is inaccessible in many of our spectra, due to the redshift range and spectral coverage of the survey. Several workers have used the EW of the [OII] λ 3727 doublet or of $H\beta$ as a star formation index for distant galaxies (e.g. Dressler & Gunn 1982; Dressler et al. 1985; Peterson et al. 1986; Broadhurst et al. 1988; Lavery & Henry 1988; Colless et al. 1990). Gallagher et al. (1989) have derived an approximate [OII] versus star formation rate (SFR) calibration from observations of [OII] and $H\beta$ in nearby blue galaxies. A direct comparison to $EW(H\alpha + NII)$ (Kennicutt 1992) showed that $EW(H\beta)$ and $EW(OIII \lambda 5007)$ can serve as good substitutes for star forming indicators in strong emission galaxies (those with $EW(H\alpha + NII) \geq 60\text{\AA}$, and $EW(H\beta) \geq 5\text{\AA}$), while $EW(OII)$ is a good indicator of star formation for all emission strengths.

The equivalent widths are measured automatically by integrating the signal above or below the local continuum outward from the center of the line until reaching the continuum level. The local continuum is determined by fitting a third order polynomial over the 350 Å on either side of the line, excluding the line itself and nearby sky lines. The algorithm

iterates the fitting 3 times while excluding the points outside 2 sigma of the continuum. The equivalent width uncertainties are calculated using Poisson statistics, the local noise in the continuum, and standard propagation of errors. The mean errors in the measurements of $\text{EW}(\text{H}\beta)$, $\text{EW}(\text{OII})$, and $\text{EW}(\text{OIII})$ are 1.8 \AA , 2.2 \AA , and 2.1 \AA respectively. Those galaxies with a continuum signal-to-noise ratio $\text{S/N} < 6$ within the 25 \AA window centered on each line are excluded from the analysis. The number of galaxies remaining for EW measurements after this S/N cut depends on the line measured; it is 18875 for the $\text{H}\beta$ line, 16377 for the $[\text{OII}]$ line and 17351 for the $[\text{OIII}]$ line.

The fibers in the du Pont multi-object spectrograph subtend a circle $3''.5$ in diameter. For galaxies with recessional velocities between 15,000 and 40,000 km s^{-1} (a velocity cut which was used for the analysis, as discussed below), this diameter corresponds to a projected circle of $5 \sim 10 \text{ kpc}$ ($H_0 = 50 \text{ km s}^{-1} \text{ Mpc}^{-1}$, $q_0 = 0.5$). This is smaller than the total size of the typical galaxy, but *much* larger than the nuclear regions, and considerably larger than the bulges of all but the most bulge-dominated galaxy. The result of this undersampling of the disks will be a small systematic underestimate of star formation rates in the earliest spirals. However, such a systematic shift will have no affect on any of the analysis presented later in this paper.

4. ENVIRONMENTAL PARAMETERS

4.1. Local Galaxy Density

To characterize the environment of LCRS galaxies, we calculate the local galaxy density, ρ , around each of the 26418 galaxies using a nearest neighbor technique. For each galaxy, we take the local galaxy density to be

$$\rho = \frac{3}{\frac{4}{3}\pi D^3} , \quad (1)$$

where D is the three-dimensional redshift-space distance from the galaxy to its third nearest neighbor. Note that this measure of galaxy density uses a three-space distance to nearest neighbors. Since the radial component of this distance is derived from the galaxy's redshift, the effect of the peculiar velocities will be spread out the neighboring galaxies along the line of sight and thus to cause a systematic underestimate of the density in the densest regions. However, in even the densest regions of the LCRS sample, we calculate the underestimate of ρ caused by the peculiar velocities to be typically less than $\sim 20 \%$, which is smaller than the width of the bins of ρ that we used for the analysis. Thus, the effect is negligible for the purpose of this study.

The effect of the variation of the survey selection function at different redshifts is removed by introducing a weight

$$w(z_i) = \frac{1}{S(z_i)} \quad (2)$$

for each galaxy i , where

$$S(z_i) = \int_{\max[M_{\min}(z_i), M_1]}^{\min[M_{\max}(z_i), M_2]} \phi(M) dM \bigg/ \int_{M_1}^{M_2} \phi(M) dM \quad , \quad (3)$$

M_1, M_2 are the absolute magnitude limits in which we are interested, and $M_{\max}(z_i)$ and $M_{\min}(z_i)$ are the absolute magnitude limits, at the redshift of galaxy i , corresponding to the apparent magnitude limits for the field containing galaxy i . We describe the differential luminosity function ϕ by a Schechter function with parameters $\phi^* = 0.019 h^3 \text{ Mpc}^{-3}$, $M_R^* = -20.29 + 5 \log h$, and $\alpha = -0.70$ (Lin et al. 1996), which we assume to be invariant with redshift.

In addition, another weight W_i is calculated for each galaxy i to take account of the field-to-field spectroscopic sampling variations. The spectroscopic completeness of a field decreases as the projected density of galaxies in the field increases, since each spectroscopic field is observed only once, using a maximum of 50 or 112 fibers. Since galaxies in denser regions were selected randomly for spectroscopy from among all galaxies meeting the photometric criteria, this effect is corrected by setting W_i to be the inverse of the fraction of spectroscopically observed galaxies in the field containing galaxy i . (Additionally, small effects from magnitude errors, apparent magnitude and surface brightness incompletenesses, and central surface brightness selection are also included in the calculated W_i . Further detailed discussions of these weights and corrections are given in Lin et al. 1996.)

Now, the corrected local galaxy density ρ around a galaxy i becomes

$$\rho_i = \frac{\sum_{j=1}^3 w(z_j) W_j}{\frac{4}{3} \pi D^3} \quad , \quad (4)$$

where j represents the rank of the nearest neighbors from galaxy i .

After removing objects too close to the LCRS survey spatial boundary, an additional conservative velocity boundary (from 15000 to 40000 km s^{-1}) was set in order to further minimize the uncertainties in the density estimate, by allowing the use of only a relatively constant selection function. The number of galaxies remaining after the velocity and spatial boundary cuts is 10536.

4.2. Membership

As a second environmental parameter, cluster or rich-group membership was determined for each galaxy in the LCRS. Cluster and rich group galaxies are defined by the three-dimensional “friends-of-friends” group identification algorithm (Huchra & Geller 1982). The algorithm finds all pairs within a projected separation D_L , and within a line of sight velocity difference V_L . Pairs with a member in common are linked into a single group. This linking makes the membership more sensitive to the environment of larger scale than the local density parameter defined in §4.1. The selection parameters D_L and V_L are scaled to account for the magnitude limit of the LCRS survey, and defined as $D_L = S_L D_0$ and $V_L = S_L V_0$. Here the linking scale S_L is calculated by

$$S_L = \left[\frac{\rho'(d_f)}{\rho'(d)} \right]^{1/3}, \quad (5)$$

where $\rho'(d)$ is the galaxy number density, at the mean comoving distance d of the galaxy pair in question, for a homogeneous sample that has the same selection function as the LCRS. In other words, $\rho'(d)$ is equivalent to the unnormalized galaxy selection function.

The distance d_f is the fiducial comoving distance at redshift z_f (we chose $cz_f=30000$ km s⁻¹) at which we define D_0 and V_0 . The density enhancement contour surrounding each group is related to D_0 by

$$\frac{\Delta\rho}{\rho} = \frac{3}{4\pi D_0^3 \rho'(d_f)} - 1 \quad (6)$$

The values of D_0 (or $\Delta\rho/\rho$) and V_0 used are taken from the LCRS group catalog (Tucker 1994; Tucker et al. 1998), and are $D_0 = 0.72 h^{-1}$ Mpc (or $\Delta\rho/\rho = 80$) and $V_0 = 500$ km s⁻¹, which are determined by several semi-quantitative constraints similar to those used in Huchra & Geller (1982), to avoid biasing the velocity dispersions of groups, and to optimize the number of interlopers.

5. RESULTS

5.1. Emission Properties of the Sample

Figure 1 presents the equivalent widths of [OII] λ 3727 and H β for 15749 LCRS galaxies; emission is represented by positive values. The majority (13951) of galaxies show negligible or weak emission, which we define to mean that EW(OII) < 20 Å and EW(H β) < 5 Å. This is the range expected of normal galaxies of types E to Sc; Kennicutt & Kent (1983) and Romanishin (1990) have shown that such galaxies have EW(H α + NII) \leq 50 Å, equivalent

to $\text{EW}(\text{OII}) \leq 20 \text{ \AA}$, assuming $\text{EW}(\text{OII}) = 0.4 \text{ EW}(\text{H}\alpha)$ (Kennicutt 1992). However, a rather significant fraction (1798 or $\sim 10\%$) of galaxies shows strong [OII] or $\text{H}\beta$ emission ($\text{EW}(\text{OII}) \geq 20 \text{ \AA}$ or $\text{EW}(\text{H}\beta) \geq 5 \text{ \AA}$), with a pattern of line strengths consistent with strong star formation activity. A typical spectrum of a strong star forming galaxy is shown in Fig. 2(a). It shows strong [OII], [OIII], and Balmer emission lines, but weak or undetectable [NeV] lines.

There is a small, fairly distinctive population (~ 30) of galaxies with [OII] emission that is weak compared to the strength of $\text{H}\beta$; typically these have $\text{EW}(\text{H}\beta) \sim 20 \text{ \AA}$ and $\text{EW}(\text{OII}) < 10 \text{ \AA}$. An example of such a spectrum is presented in Figure 2(b). These galaxies show strong broad Balmer emission lines, strong [OIII] emission, but weak emission in [OII]; most are Seyfert 1 galaxies (Kennicutt 1992).

Another group of ~ 40 galaxies shows relatively strong [OII] emission, independent of Balmer line strength (most of these occupy the upper left corner of Fig. 1). A typical spectrum (Fig. 2(c)) shows that these galaxies have strong [OIII] emission with respect to Balmer emission, in addition to strong [OII] emission. These spectra are also often accompanied by [NeV] $\lambda 3425$ emissions and are suspected to be mostly Seyfert 2's or LINER's (Kennicutt 1992).

5.1.1. Emission Classes

For the analysis which follows, it is convenient to divide the galaxies into classes of emission line strength. We use the [OII] equivalent width, and define three classes: *no emission* or NEM, for which $\text{EW}(\text{OII}) < 5 \text{ \AA}$, *weak emission* or WEM, for which $5 \text{ \AA} \leq \text{EW}(\text{OII}) < 20 \text{ \AA}$, and *strong emission*, or SEM, for which $\text{EW}(\text{OII}) \geq 20 \text{ \AA}$.

Assuming $\text{EW}(\text{OII}) = 0.4 \text{ EW}(\text{H}\alpha)$ (Kennicutt 1992), the $\text{EW}(\text{OII}) = 20 \text{ \AA}$ upper boundary of the WEM class corresponds to $\text{EW}(\text{H}\alpha) = 50 \text{ \AA}$. This boundary is where Kennicutt & Kent (1983) found the upper limit of $\text{EW}(\text{H}\alpha)$ for the normal spirals. Thus, it is plausible that the WEM galaxies are predominantly “normal” galaxies, in which star formation is governed by *internal* factors such as gas content and disk kinematics.

In contrast to these, Kennicutt et. al (1987) found that galaxies with $\text{EW}(\text{H}\alpha) \geq 50 \text{ \AA}$ are usually members of close pairs and suggested that their star formation rates are only weakly correlated with their internal properties, and much more correlated with external influence. In fact, many studies suggest that a large fraction of “starburst” galaxies are members of interacting systems (e.g., Heidmann and Kalloghlian 1973; Wasilewski 1983), and therefore that interactions of galaxies are one of the important triggering mechanisms

for starbursts. If this is correct, and if starbursts predominate in the SEM class, the variation with environment of the fraction of SEM galaxies may reflect environmental variations in galaxy interaction rates.

5.1.2. AGNs

Using EW(OII) as an indicator of the SFR fails for galaxies with luminous active nuclei (AGNs) (Kennicutt 1992). Thus, excluding AGNs is desirable, even if the total number of AGNs is minimal, particularly if AGN activity has a different dependence on environment than does star formation activity. AGN galaxies fall into two classes, those with abnormally strong [OII] emission, independent of Balmer line strength, and those with strong Balmer, and [OIII] emission but weak emission in [OII]. The former most often are Seyfert 2 or LINER, and the latter tend to be Seyfert 1, though there are exceptions to this rule (Kennicutt 1992).

Seyfert 1 galaxies are relatively easy to identify. With their weaker [OII] emission with respect to the $H\beta$ emission, and their broad Balmer lines, Seyfert 1 galaxies are a distinctive population among emission galaxies in the EW(OII) vs. EW($H\beta$) plane. We exclude 33 galaxies from the sample with $EW(H\beta) \geq 7 \text{ \AA}$ and $EW(OII) \leq 15 \text{ \AA}$, all of whom show broad Balmer emission lines. Identifying Seyfert2's or LINER's is somewhat less reliable using the EW(OII) vs. EW($H\beta$) plane alone, without access to the $H\alpha$ line. We did our best by additionally using EW(OIII) and EW(NeV($\lambda 3425$)) to exclude a larger subset of 45 galaxies which *includes* Seyfert2/LINER galaxies, but also probably some non-AGNs, using the criteria $EW(OIII)/EW(H\beta) \geq 2$ or $EW(NeV(\lambda 3425)) \geq 7 \text{ \AA}$.

5.2. Morphology

The goal of this paper is to investigate how star formation rates within galaxies vary with environment. However, the star formation rate in galaxies, in the weak star formation regime in particular, is generally correlated with their morphological type (Kennicutt & Kent 1983). Moreover, the distribution of morphological type itself is a function of environment (Dressler 1980). Thus, comparison of star formation rates among environmental subsets needs to account for any differences in the morphological distribution among the galaxy subsets.

Our task is, however, complicated by the fact that the star formation rate is one of the parameters which *define* the morphological type. In the Hubble System (Sandage 1961),

morphological type is based on three characteristics: bulge-to-disk ratio (B/D), tightness of spiral arms, and the degree of resolution of spiral arms. It is widely believed that the tightness of spiral arms is related to the mass distribution within a galaxy, and therefore to B/D. The degree of resolution of spiral arms is, on the other hand, strongly affected, even defined, by the star formation activity in the arms. Thus, two (rather than one) physical parameters, star formation rate and mass distribution, map into three parameters characterizing the Hubble System, and this star formation dependency of the Hubble System complicates our analysis.

The reason is straightforward to understand. If a particular environment reduces the SFR in a galaxy, this decrease in SFR will shift its Hubble type towards an earlier type. Because the galaxy appears with an earlier Hubble type, we will *expect* a lower SFR, and therefore underestimate the amount by which star formation has been diminished. The result is a lowered sensitivity to environmental changes in SFR. Van den Bergh (1976), who introduced the term ‘anemic’ to refer to galaxies with weak star formation, in a way recognized this dangerous star formation dependence of the Hubble type. However, the better cure is using a measure of galaxy morphology which is *independent* of SFR. From the earlier discussion of the Hubble sequence, it is clear that the natural candidate is mass distribution, but that can only be determined from rotation curves, and is, therefore, an impractical measure for any large sample of galaxies. A more practical measure is the light distribution.

We quantify the light distribution of the LCRS galaxies using the automatically-determined concentration index C (Okamura, Kodaira, & Watanabe 1983; Doi, Fukugita, & Okamura 1993; Abraham et al. 1994), which measures the intensity-weighted second moment of the galaxies and compares the flux between the inner ($r < 0.3$) and outer ($r < 1$) isophote to indicate the degree of light concentration in the galaxy images. Here r is a normalized radius which is constant on an elliptical isophote and is normalized in such a way that r is unity when the area within the ellipse is equal to the detection area of a galaxy. (For further details of the definition, please see Abraham et al. 1994.)

The concentration index C has been developed as a substitute for Hubble type, however, we stress that C actually has a significant advantage over Hubble type for the purpose of investigations of star formation. In other words, it is as a purer measure of one of the two physical parameters determining Hubble type that we make use of it. Concentration not only suits our needs better than Hubble type, it is also more robust against image degradation, and also easier to be measured automatically. It is, thus, ideal for a large galaxy survey, such as the LCRS, where the sample size is $\sim 10^4$ and most of the galaxies consist of on the order of 10^2 resolution elements. (Image parameters of LCRS

galaxies are further discussed in Hashimoto et al. 1998).

In Figure 3 we present the relation between C and mean [OII] equivalent width of the galaxies in our sample. This figure shows a smooth increase in mean EW with decreasing C which parallels the relation between the Hubble type and $EW(H\alpha)$ (e.g. Kennicutt & Kent 1983), or $EW(OII)$ (Kennicutt 1992). This is the relationship which we shall use as a baseline for the comparison of the star formation rates. Figure 4 shows the distribution of C in each of the three emission classes. The distribution for the WEM class is more skewed toward late/irregular type galaxies (smaller C) than is that of the NEM class, as one would expect. The SEM class, on the other hand, shows a C distribution roughly identical to that of the WEM class, suggesting that the influence of mass distribution, or “galactic structure”, is minimal here. Thus, differences between the SEM and WEM classes must be due entirely to factors other than galactic structure.

5.3. Correlation with Local Density

5.3.1. Density effects in the field

Figure 5 shows the SEM/WEM and WEM/NEM population ratios as a function of the local space density for the LCRS sample. Bars are root N error. *The small difference in the C distribution between SEM and WEM shown in Fig. 4 has been removed in order to ensure that the population difference with respect to the density does not come from an indirect result of a correlation of galactic structure with density.* The correction is made by assigning a weight to each WEM galaxy in a given C bin so that the sum of the weight of WEM galaxies in that C bin will be equal to the total *number* of SEM galaxies in the same C bin. All WEM galaxies in one C bin carry exactly the same weight and this weight, instead of the count, is used for WEM galaxies throughout the population analyses. A similar correction is made between WEM and NEM by assigning weights to NEM galaxies to match the C distribution of the WEM class.

Emission line strengths are sometimes found to be correlated with galaxy luminosity, in the sense that galaxies of lower luminosity exhibit stronger emission (e.g. Kennicutt & Kent 1983; Kennicutt et. al 1984). This trend, however, is primarily due to the correlation of absolute magnitude with morphological type: late-type galaxies tend to be both less luminous and exhibit stronger star formation. Since we applied the correction using C , this luminosity bias is mostly removed. As an extra precaution, however, to ensure that we have no EW biases with respect to redshift, we further remove any difference in the distributions of absolute R magnitudes between SEM & WEM, or WEM & NEM, by

assigning additional weights to WEM or NEM galaxies, until the shapes of their absolute magnitude distributions match that of SEM or WEM galaxies, respectively. (Hereafter, whenever the correction using C is applied, it is always accompanied by an additional absolute magnitude correction.)

Figure 5 shows the correlation between the local density and the population ratios of different emission types. Fig. 5a shows the population ratio of SEM to the WEM emission class versus the local galaxy space density (ρ), while Fig. 5b shows the corresponding ratios of WEM to NEM galaxies. Both Fig. 5a & b show a decrease in emission line strength as density increases, although the trend is stronger in Fig. 5b.

Fig. 5 includes both cluster and field galaxies. Since different processes may be operating, with different effect, inside and outside of clusters, it is necessary to examine each population separately. We define “cluster galaxies” by the method outlined in §4. Meanwhile, galaxies outside clusters, hereafter “field galaxies”, are identified by removing cluster galaxies from the entire sample, except that this time, a lower $\Delta\rho/\rho=40$ contour is used to ensure that galaxies in the outskirts of clusters are excluded from the field sample. Note that the “field” galaxies do not necessarily consist entirely of so called “isolated” galaxies, those without any physical associations to which the galaxy belongs. Some of our field galaxies may be members of low density associations, such as loose groups.

Fig. 6 shows the population ratios similar with Fig. 5, but now for the *field* sample alone. Overall, Fig. 6 still shows qualitatively the same correlation as Fig. 5, namely, galaxies with higher emission tend to be more abundant in less dense environments. However, unlike Fig. 5, the SEM/WEM comparison (Fig. 6a) shows a stronger correlation than the WEM/NEM one (Fig. 6b). In particular, in Fig. 6b, the slope is rather flat compared to Fig. 6a (and Fig. 5b), except for the lowest density regime. Meanwhile, Fig. 6a shows a clear trend of stronger emission galaxies becoming more prevalent in less dense environments.

5.3.2. Density effects in clusters

Fig. 7 shows the same relation as Fig. 6 for the cluster and rich group (hereafter “cluster”) sample, alone. Overall, again, Fig. 7 shows a qualitatively similar correlation as that in Fig. 6: galaxies with stronger emission lines prefer less dense environments. Fig. 7a, however, is less conclusive due to the small number of emission line (particularly SEM) galaxies inside clusters. Meanwhile, Fig. 7b shows a clear trend of galaxies with no emission lines becoming more prevalent in denser environments. This is rather interesting, especially

comparing this to the previously shown (Fig. 6b) weak correlation of WEM/NEM in the field sample. Since the WEM/NEM ratio is expected to measure the extent of “normal” star formation, this fact might suggest that the mechanism affecting normal star formation might operate more efficiently in the cluster environment, than in the field.

5.4. Comparison between Clusters and Field

Figure 8 shows the distribution of C for cluster and field galaxies. The solid line represents cluster galaxies, while the dotted-dashed line represents galaxies in the field. The C distribution of the cluster galaxies is skewed toward early type (larger C), consistent with the well-established trend towards larger-bulge systems inside clusters.

Figure 9 shows the cumulative EW(OII) distribution for the cluster and field sample, after application of a C correction similar to that in §5.3, except that weights are now assigned to field galaxies, in order to match the C distribution of the field sample to that of the cluster sample. The two distributions in Figure 9 indicate that field galaxies tend to have higher EW(OII) than cluster galaxies. A Kolmogorov-Smirnov (KS) test shows that the probability that the two distributions are drawn from the same parent distribution is only 5×10^{-21} .

Figure 9 includes galaxies of all “structural” types. Since the processes leading to the cluster/field differences exhibited here might operate differently on different type galaxies, we split the sample into three C subclasses. Figure 10 shows the same plot as Figure 9 for the three separate C bins, $0.35 < C \leq 0.5$, $0.25 < C \leq 0.35$, and $0.1 < C \leq 0.25$. (The field/cluster C correction is applied within each subclass.) Though the effect is somewhat weaker than in Figure 9, all three bins of Figure 10 still show the same trend, namely that field galaxies tend to show higher [OII] emission than cluster galaxies. KS probabilities for the three bins are 3×10^{-9} , 1×10^{-14} , and 4×10^{-3} , respectively. We do not, however, find any strong qualitative differences among the three C bins.

A different look at the same trends is presented in Table 1, which lists the percentiles of the various emission classes in different environments. The emission classes are defined in the same way as in §5.1, except that the SEM class is further subdivided into a low subset (LSEM) and a high subset (HSEM) at the border $\text{EW(OII)} = 50 \text{ \AA}$. The C corrections have *not* been applied in Table 1. Cluster and field definitions are the same as in §4.2 and §5.3. Additionally, rich and poor cluster subsets are introduced, defined by their total luminosities L_T , which have been calculated as described in Tucker (1994). Rich clusters are defined as clusters with $L_T \geq 5 \times 10^{11} L_\odot$, while poor clusters are clusters with $L_T \leq 0.5 \times 10^{11} L_\odot$.

Also included in Table 1 are 1σ uncertainties, calculated from Poisson statistics. The numbers in parentheses are the total number of galaxies in each environmental class.

Table 2 repeats the analysis of Table 1, but with C corrections. The corrections were made using the same method as in §5.3, now applied to match the C distributions of the field, rich clusters, and all-cluster samples to the C distribution of the poor cluster class. Although there are small differences between the numbers in the two tables, the same trends are apparent. As was evident from Figures 9 and 10, star formation rates are higher in the field than in clusters. However, dividing clusters into rich and poor systems reveals some remarkable complexities underlying this general trend. Rich clusters show a somewhat depressed level of “normal” star formation, as counted by the WEM fraction: a factor of 2 relative to field galaxies, and a factor of 1.4 when C corrections are made. However, the frequency of starbursts, as counted by the LSEM and HSEM fractions, is depressed by much more: a factor of about 5 relative to the field.

Most remarkable are the percentiles in the poor clusters. Poor clusters show *higher* levels of star formation than even the field. This enhanced star formation is particularly evident at the highest star formation rates: the HSEM galaxies are almost 4 times more abundant in poor clusters than in any other population. A χ^2 test shows that the proportions for the poor cluster galaxies and the field galaxies are significantly different at significance level $\alpha = 2 \times 10^{-4}$ for the HSEM class.

6. DISCUSSION

The results of this study can be summarized as follows:

- (1) The correlation between the two fundamental physical parameters underlying the Hubble sequence, star formation rate and bulge-to-disk ratio, varies with environment.
- (2) Cluster galaxies exhibit *reduced* star formation compared to the field control sample of the same concentration index, or “galactic structure”. We did not find any qualitatively different responses to environments between early and late type spirals, which some previous researches reported.
- (3) Star formation rate of galaxies of a given “galactic structure” is sensitive to local galaxy density and shows a continuous correlation with the local density, in such a way that galaxies show higher levels of star formation in low density than in high density environments. Remarkably, this trend is also observed both inside and outside of clusters, implying that physical processes responsible to this correlation might not be intrinsic to

cluster environments.

(4) Among field populations, the abundance of strong emission line galaxies, or “starburst” galaxies, is more sensitive to local density than the abundance of weak emission line galaxies, i.e. “normal star formation” galaxies. Among cluster populations, the opposite is true.

(5) While rich clusters show lower levels of “normal star formation”, and much lower levels of “starbursts” than the field, poor clusters show enhanced levels of both. The starburst level in poor clusters is a factor of four higher than that in either the field or rich clusters.

Reviewing these results, one might be tempted to conclude that star formation rates are higher in low density than in high density environments and that the field/cluster difference is simply a manifestation of the variation of SFR with local density. However, a comparison of Figures 7 and 6 shows that things are not this simple. At low levels of star formation, the SFR is quite sensitive to density inside clusters, but only weakly dependent on density in the field. However, this is not the case for galaxies with high levels of star formation, which appear to be at least as sensitive to local density in the field as in clusters. Even this description is an oversimplification. Table 2 demonstrates that the variation of SFR with environment is not monotonic. The highest levels of star formation are more prevalent in the intermediate environment of poor clusters than in either the field or rich clusters.

It is clear from these, as well as many earlier findings, that environment has a profound effect not only on the structure but also on the star formation rates within galaxies. Popular ideas about the effect of environment on galactic star formation envision at least two kinds of processes at work: those that lower the gas content, and therefore the potential star formation rate in galaxies, and those that precipitate bursts of star formation. Among the former are interactions between the intragalactic and intergalactic media, including stripping and evaporation (Gunn & Gott 1972; Cowie & Songaila 1977), tidal interactions which remove gas from disks (e.g. Spitzer & Baade 1951; Valluri & Jog 1990), and the suppression of infall of new gas-rich material from outside the galaxy (Larson, Tinsley, & Caldwell 1980). Among the latter are tidal shocks (e.g. Noguchi & Ishibashi 1986, Sanders et al. 1988), ram pressure induced star formation (Dressler & Gunn 1983), and mergers with other systems (e.g. Bares & Hernquist 1991).

Our understanding of all these processes is incomplete, and their effects may be complex. Tidal encounters and galaxy “harassment” (Moore et al. 1996) might either enhance or depress average star formation rates. More generally, short-term *increases*

in star formation rate will deplete the gas supply at a higher rate, leading, perhaps, to longer-term *decreases* in star formation. Nevertheless, there are some generalizations which it is probably safe to make. Ram pressure and evaporative stripping of gas is a process which depends on a dense and/or hot intergalactic medium, and therefore only works well only in rich clusters. Mergers of gas-rich systems, which probably produce starbursts, depend on the galaxy-galaxy encounter rate. Encounters between galaxies will be more prevalent in denser, and higher velocity dispersion environments, but such encounters will only lead to mergers if the relative velocities of the galaxies are comparable to or lower than the characteristic velocities within the galaxies.

One can combine these generalizations with our previous inferences that the WEM galaxies are undergoing “normal” star formation and the SEM galaxies are undergoing starbursts to produce a picture which is facile and oversimplified but may be basically true. This picture predicts that the WEM/NEM ratio, measuring normal star formation, should decline with density, particularly in rich clusters, which it does. It also predicts that the SEM fraction, measuring starbursts, should increase with density until the local velocity dispersion exceeds internal galaxy velocities, after which it should drop. As a result, groups and poor clusters should have the highest proportion of SEM galaxies, which they do.

This may be too easy a solution. A rough correspondence of expectations and observed trends does not prove that gas stripping and encounter-driven starbursts are responsible for the environmental effects on star formation rates that we observe. However, whatever the real processes at work, we *can* confidently conclude that they number at least two: one which suppresses star formation in clusters, and one which precipitates starbursts in intermediate density environments. Thus, one of the two fundamental galactic parameters, star formation rate, is profoundly affected by galaxies’ environments. To what extent the other fundamental parameter, structure, is also a product of environment will be the subject of following papers.

We thank Richard Larson and Richard Ellis for their useful suggestions and Ian Smail for kindly providing his codes. YH acknowledge Becky Koopmann for helping the manuscript. This work was partially supported by NSF grant AST91-15446. The Las Campanas Redshift Survey was supported by NSF grants AST87-17207, AST89-21326, and AST92-20460. YH was partially supported by a Carnegie Predoctoral Fellowship.

REFERENCES

- Abraham, R. G., Valdes, F., Yee, H. K. C., & van den Bergh, S. 1994, *ApJ*, 432, 75
- Allington-Smith, J. R., Ellis, R. S., Zirbel, E. L., & Oemler, A. 1993, *ApJ*, 404, 521
- Barnes, J. E., & Hernquist, L. E. 1991, *ApJ*, 370, L65
- Bhavsar, S. 1981, *ApJ*, 246, L5
- Broadhurst, T. J., Ellis, R. S., & Shanks, T. 1988, *MNRAS*, 235, 827
- Butcher, H. R., & Oemler, A. 1985, *ApJ*, 285, 426
- Byrd, G., & Valtonen, M. 1990, *ApJ*, 350, 89
- Colless, M., Ellis, R. S., Taylor, K., & Hook, R. N. 1990, *MNRAS*, 244, 408
- Cowie, L. L., & Songaila, A. 1977, *Nature*, 266, 501
- de Souza, R.E., Capelato, H.V., Arakaki,L., and Logullo, C. 1982, *ApJ*, 263, 557
- Doi, M., Fukugita, M., Okamura, S. 1993, *MNRAS*, 264, 832
- Dressler, A. 1980, *ApJ*, 236, 351
- Dressler, A., & Gunn, J. E. 1982, *ApJ*, 263, 533
- Dressler, A., & Gunn, J. E. 1983, *ApJ*, 270, 7
- Dressler, A., Thompson, I. B., & Shectman, S. A., 1985, *ApJ*, 288, 481
- Dressler, A., Gunn, J. E., & Schneider, D. P. 1985, *ApJ*, 294, 70
- Dressler, A., Oemler, A., Butcher, H. R., & Gunn, J. E. 1994, *ApJ*, 430, 107
- Gallagher, J. S., Bushouse, H., & Hunter, D. A. 1989, *AJ*, 97, 700
- Gavazzi, G., & Jaffe, W. 1985, *ApJ*, 294, L89
- Giovanelli, R., Haynes, M.P., and Chincarini, G.L. 1986, *ApJ*, 300, 77
- Gisler, G. R. 1978, *MNRAS*, 183, 633
- Glazebrook, K., Ellis, R., Colles, M., Broadhurst, T., Allington-Smith, J., & Tanvir, N. 1995, *MNRAS*, 273, 157

- Gunn, J. E., & Gott, J. R. 1972, ApJ, 176, 1
- Hashimoto, Y., Oemler, A., & Tucker, D. L., 1998, in preparation
- Heidmann, J., & Kalloghlian, A. T. 1973, Astrofizika 9, 71
- Huchra, J. P., & Geller, M. J. 1982, ApJ, 257, 423
- Keel, W. C., Kennicutt, R. C., Hummel, E., & van der Hulst, J. M. 1985, AJ, 90, 708
- Kennicutt, R. C. 1983, ApJ, 272, 54
- Kennicutt, R. C. 1992, ApJ, 388, 310
- Kennicutt, R. C., Bothun, G. D., & Schommer, R. A. 1984, AJ, 89, 1279
- Kennicutt, R. C., Keel, W. C., van der Hulst, J. M., Hummel, E., & Roettiger, K. A., 1987, AJ, 93, 1011
- Kennicutt, R. C., & Keel, W. C. 1984, ApJ, 279, L5
- Kennicutt, R. C., & Kent, S. M. 1983, AJ, 88, 1094
- Larson, R. B., Tinsley, B. M., & Caldwell, C. N. 1980, ApJ, 237, 692
- Lavery, R. J., & Henry, J. P. 1988, ApJ, 330, 596
- Lilly, S. J., Le Fevre, O., Hammer, F. & Crampton, D. 1996, ApJ, 460, L1
- Lin, H., Kirshner, R. P., Shectman, S. A., Landy, S. D., Oemler, A., Tucker, D. L., and Schechter, P. L., 1996 ApJ, 464, 60
- Moore, B., Katz, N., Lake, G., Dressler, A., & Oemler, A. 1996, Nature, 379, 613
- Moss, C., & Whittle, M. 1993, ApJ, 407, L17
- Noguchi, M., & Ishibashi, S. 1986, MNRAS, 219, 305
- Okamura, S., Kodaira, K., & Watanabe, M. 1984, ApJ, 280, 7
- Peterson, B. A., Ellis, R. S., Bean, A. J., Efstathiou, G., Shanks, T., Fong, R., & Zou, Z.-L. 1986, MNRAS, 221, 233
- Postman, M., and Geller, M. J. 1984, ApJ, 281, 95
- Romanishin, W. 1990, AJ, 100, 373

- Sandage, A. 1961, ApJ, 133, 355
- Sanders, D. B., Soifer, B. T., Elias, J. H., Madore, B. F., Matthews, K., Neugebauer, G., & Scoville, N. Z. 1988, ApJ, 325, 74
- Shectman, S. A., Schechter, P. L., Oemler, A., Tucker, D. L., Kirshner, R. P., and Lin, H. 1996, ApJ, 470, 172
- Spitzer, L. & Baade, W. 1951, ApJ, 113,413
- Tucker, D. L. 1994, Ph.D. Thesis, Yale University
- Tucker, D. L., Oemler, A., Hashimoto, Y., Kirshner, R. P., Lin, H., Shectman, S. A., Landy, S. D., & Schechter, P. L. 1998, in preparation
- Tully, R. B. 1988, AJ, 96, 73
- Valluri, M., & Jog, C. 1990, ApJ, 357, 367
- van den Bergh, S. 1976, ApJ, 206, 883
- Wasilewski, A. J. 1983, ApJ, 272, 68
- Whitmore, B. C., & Gilmore, D. M. 1991, ApJ, 367, 64

Fig. 1.— The distribution of equivalent widths of 15749 LCRS galaxies in the $[\text{OII}]\lambda 3727$ versus $\text{H}\beta$ plane, where the emission is represented by positive values.

Fig. 2.— Optical spectra of galaxies with strong emission lines. (a) Typical strong star-forming galaxies (b) Typical spectrum of Seyfert 1. (c) Typical spectrum of Seyfert2/LINER. Wavelength is in the observed frame.

Fig. 3.— Relationship between the concentration index (C ; Abraham et al. 1994) and mean equivalent width of $[\text{OII}]\lambda 3727$ for 16377 LCRS galaxies. It shows a smooth increase in the mean of EW with decreasing C , which parallels the relation between the Hubble type and $\text{EW}(\text{H}\alpha)$ (e.g. Kennicutt & Kent 1983), or $\text{EW}(\text{OII})$ (Kennicutt 1992)

Fig. 4.— Distribution of the concentration index, C in the three emission classes; SEM ($\text{EW}(\text{OII}) \geq 20 \text{ \AA}$), WEM ($5 \text{ \AA} \leq \text{EW}(\text{OII}) < 20 \text{ \AA}$), and NEM ($\text{EW}(\text{OII}) < 5 \text{ \AA}$) as defined in §5.3

Fig. 5.— Correlation between the local space density and the population of different emission classes for LCRS galaxies. The difference in the morphological distributions between the emission classes are corrected using the concentration index, C . (a) SEM/WEM population ratio as a function of the local space density. (b) WEM/NEM population ratio as a function of the local space density. Bars are root N error.

Fig. 6.— Correlation between the local space density and the population of different emission classes for *field* subsets. The C correction is also applied.

Fig. 7.— Correlation between the local space density and the population of different emission classes for *cluster* subsets, after the C correction.

Fig. 8.— Distribution of the concentration index C of the cluster galaxies and the field galaxies. The solid line represents cluster galaxies, while the dotted-dashed line represents galaxies in the field. The C distribution of the cluster galaxies is skewed toward early type (larger C), consistent with the well-established trend towards larger-bulge systems inside clusters.

Fig. 9.— Fig. 9 shows the cumulative $\text{EW}(\text{OII})$ distribution for the cluster and field sample, after application of the C correction. The two distributions indicate that field galaxies tend to have higher $\text{EW}(\text{OII})$ than cluster galaxies.

Fig. 10.— The same plot as Fig. 9 for three separate C bins, $0.35 < C \leq 0.5$, $0.25 < C \leq 0.35$, and $0.1 < C \leq 0.25$. (The C correction is also applied.) Though the effect is somewhat weaker than in Fig. 9, all three bins of Fig. 10 still show the same trend, namely that field

galaxies tend to show higher [OII] emission than cluster galaxies.

Table 1. Percentiles of Emission Classes

Class	Field (6051)	Cluster Poor (346)	Cluster All (3825)	Cluster Rich (394)
NEM	56.8±0.6	43.6±2.7	68.7±0.8	80.5±2.0
WEM	33.1±0.6	39.6±2.6	24.6±0.7	17.6±1.9
LSEM	9.1±0.3	13.8±1.8	5.9±0.3	1.5±0.6
HSEM	0.9±0.1	3.0±0.8	0.8±0.1	0.4±0.3

Table 2. Percentiles of Emission Classes (with C Correction)

Class	Field	Cluster Poor	Cluster All	Cluster Rich
NEM	55.3±2.6	43.6±2.7	62.8±2.6	73.9±2.4
WEM	33.5±2.5	39.6±2.6	29.2±2.4	23.9±2.3
LSEM	10.3±1.6	13.8±1.8	6.9±1.4	1.5±0.7
HSEM	0.8±0.4	3.0±0.8	1.0±0.5	0.7±0.4

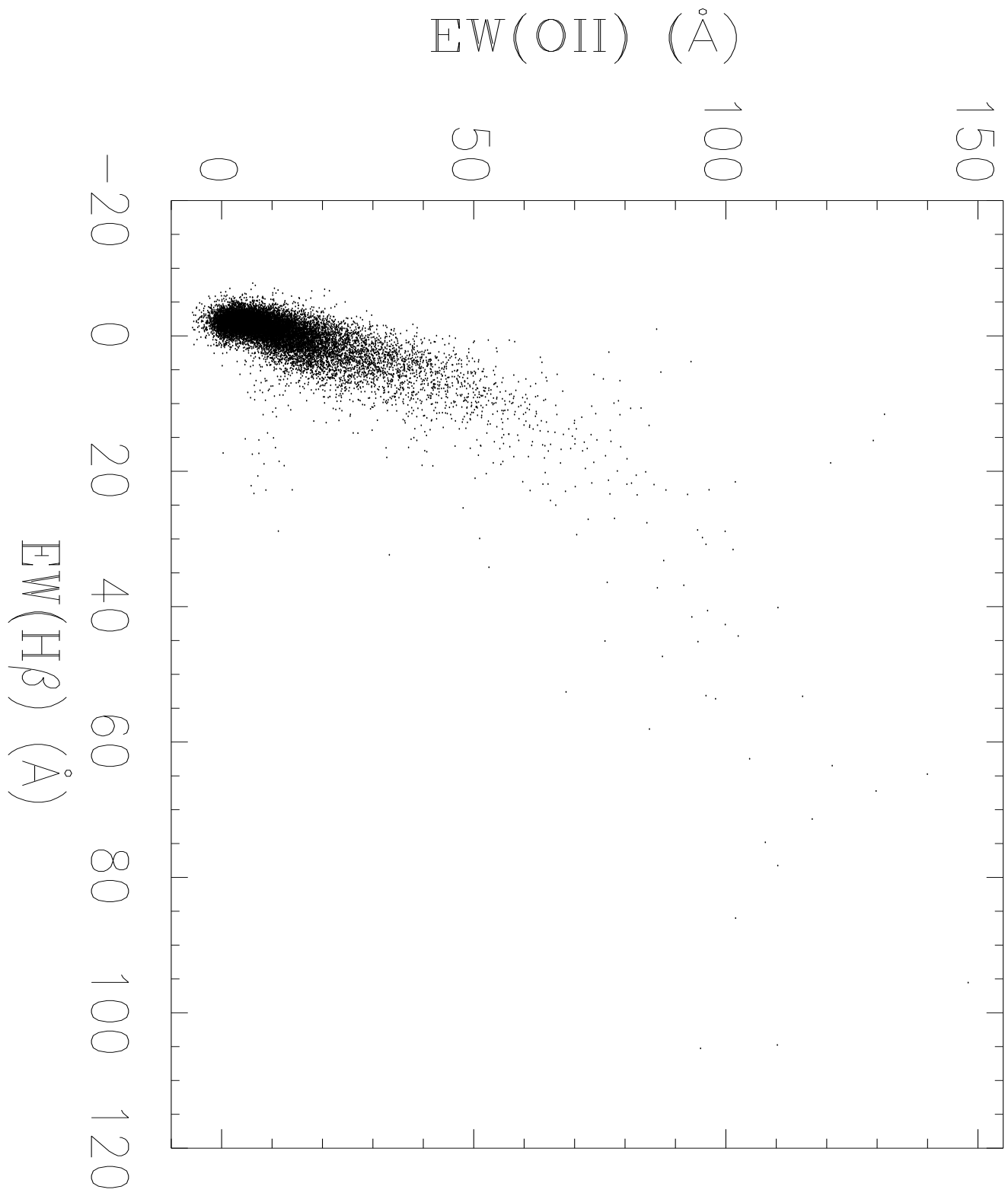


Fig. 1

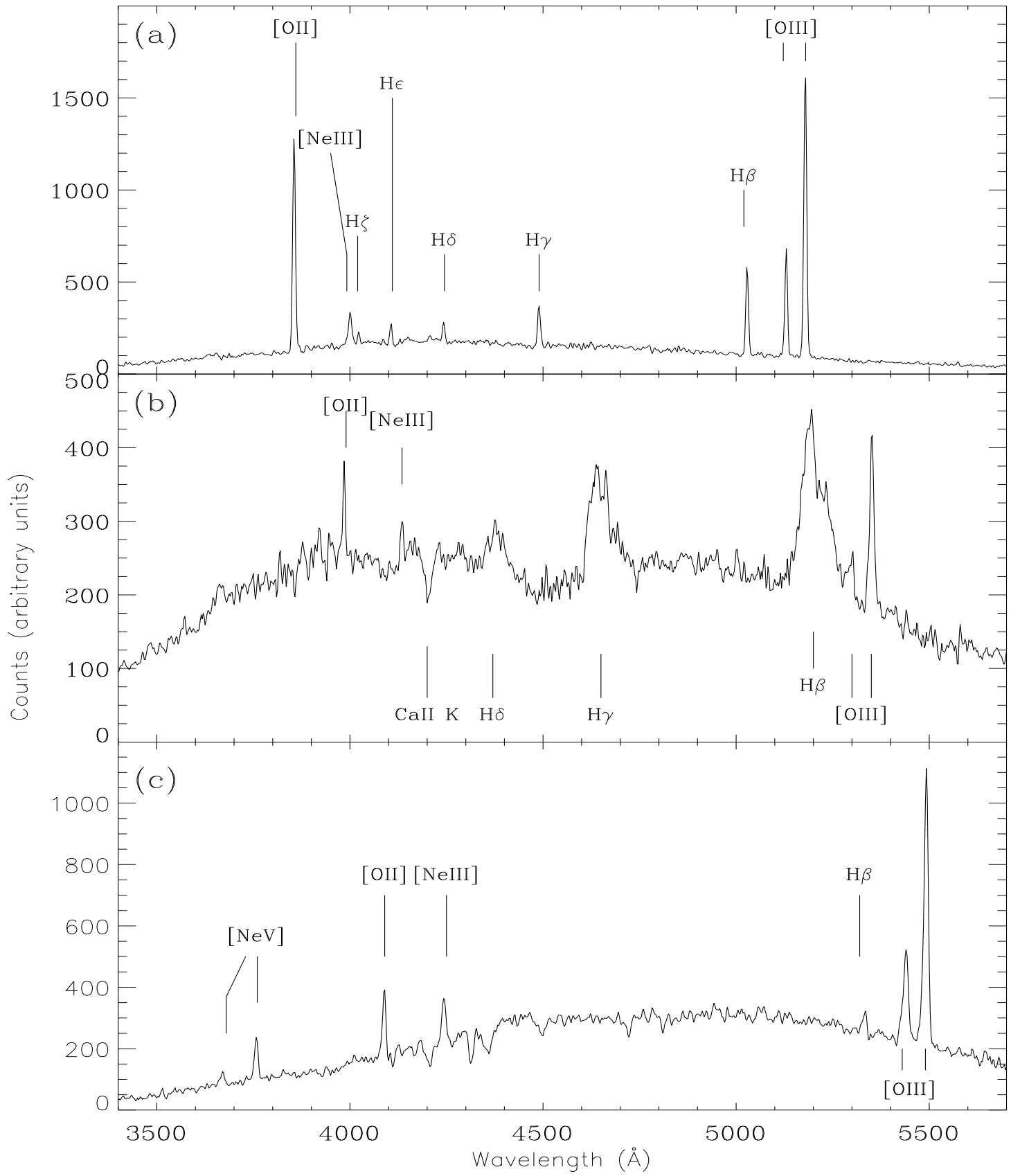


Fig. 2

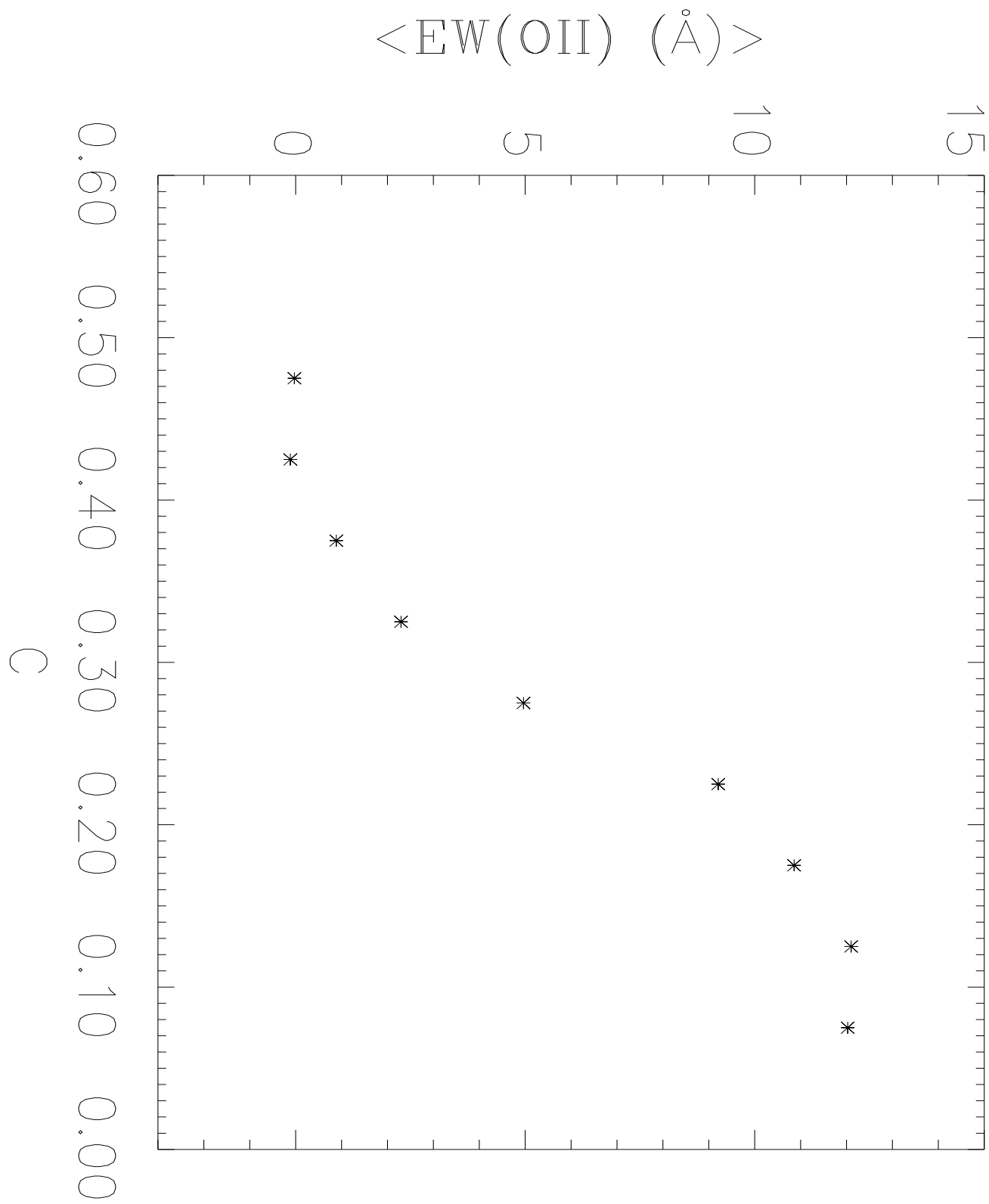


Fig. 3

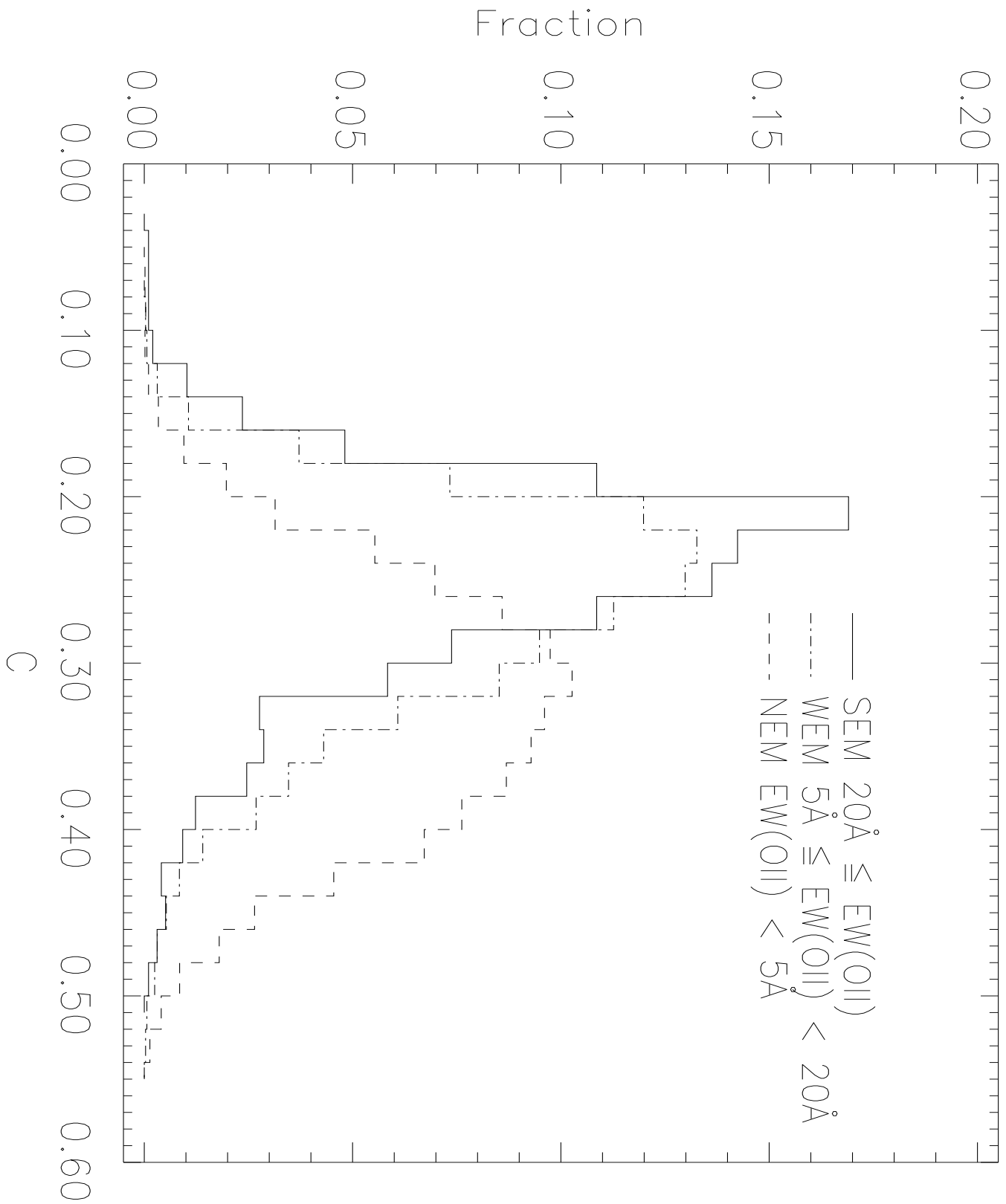


Fig. 4

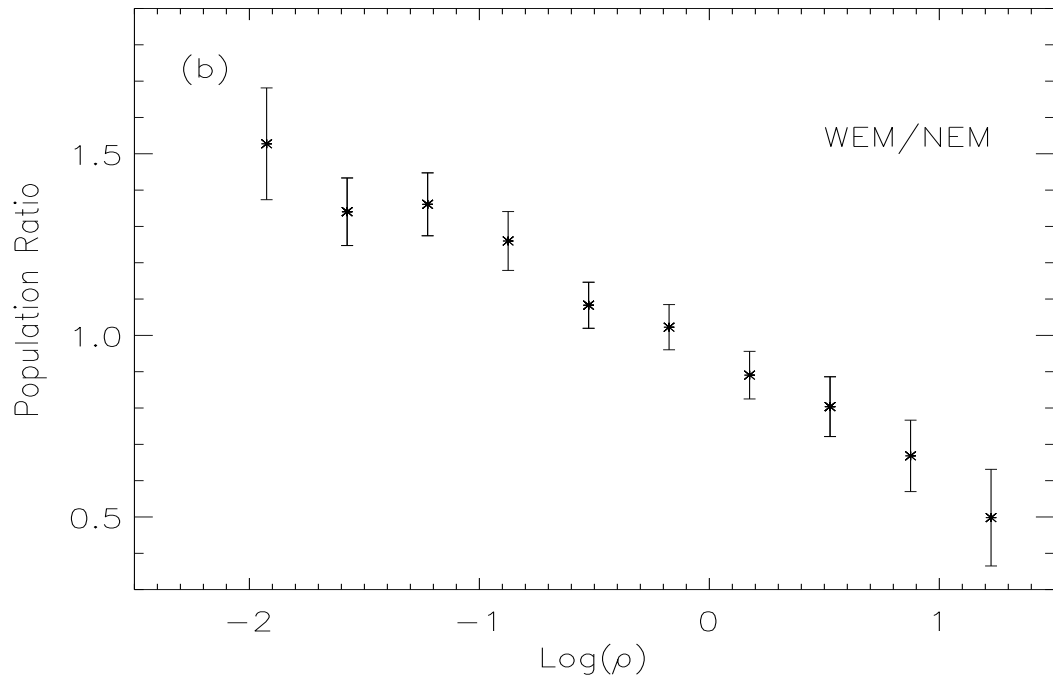
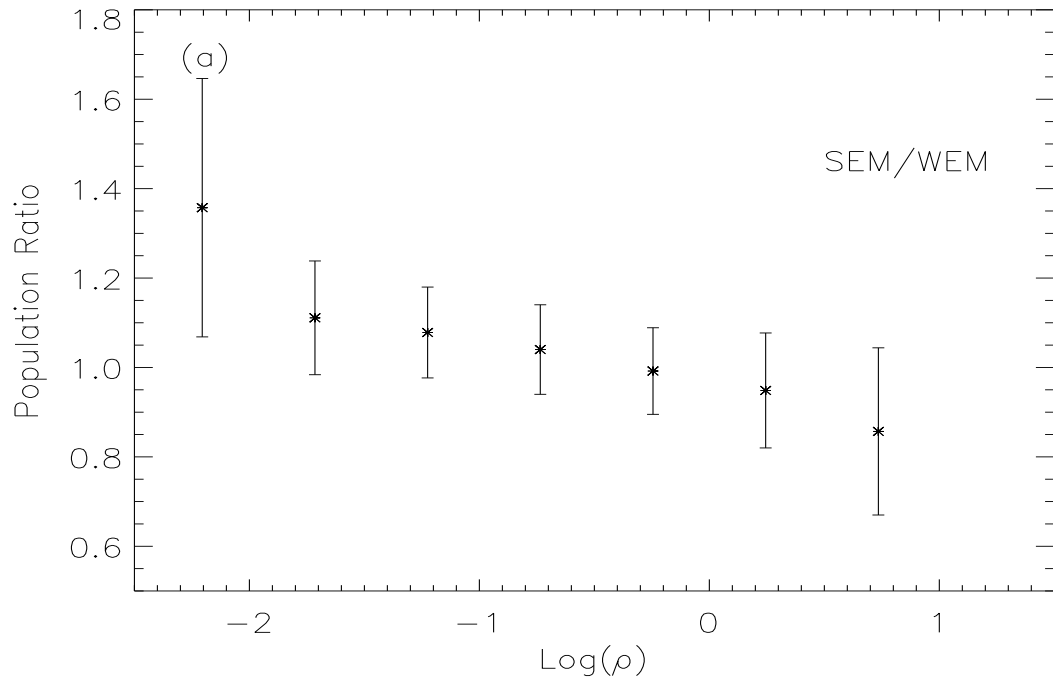


Fig. 5

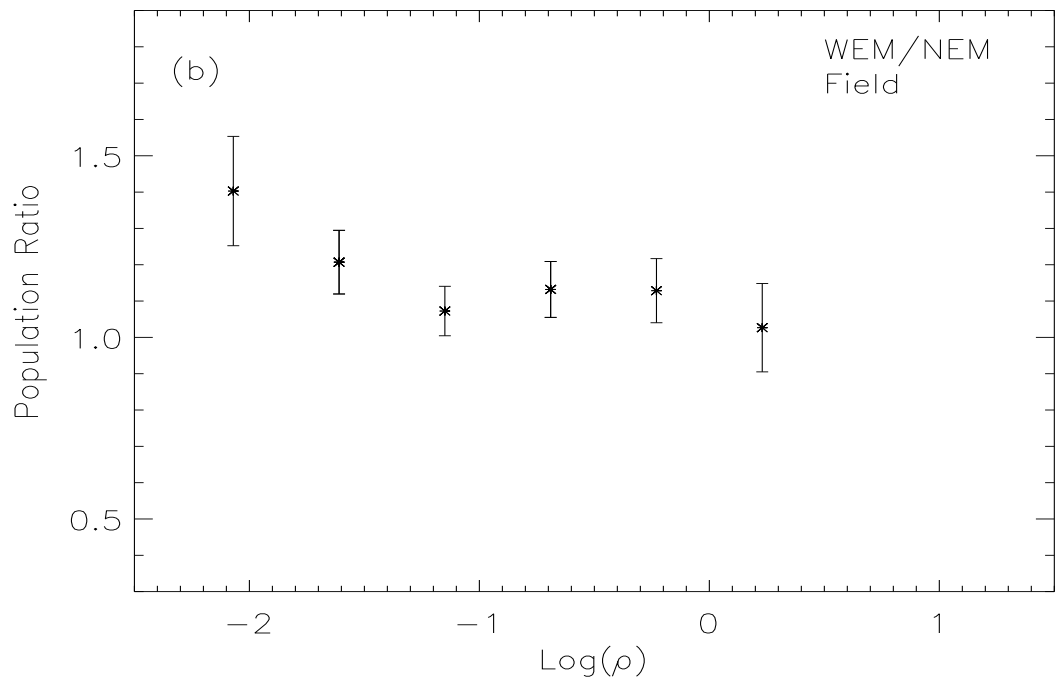
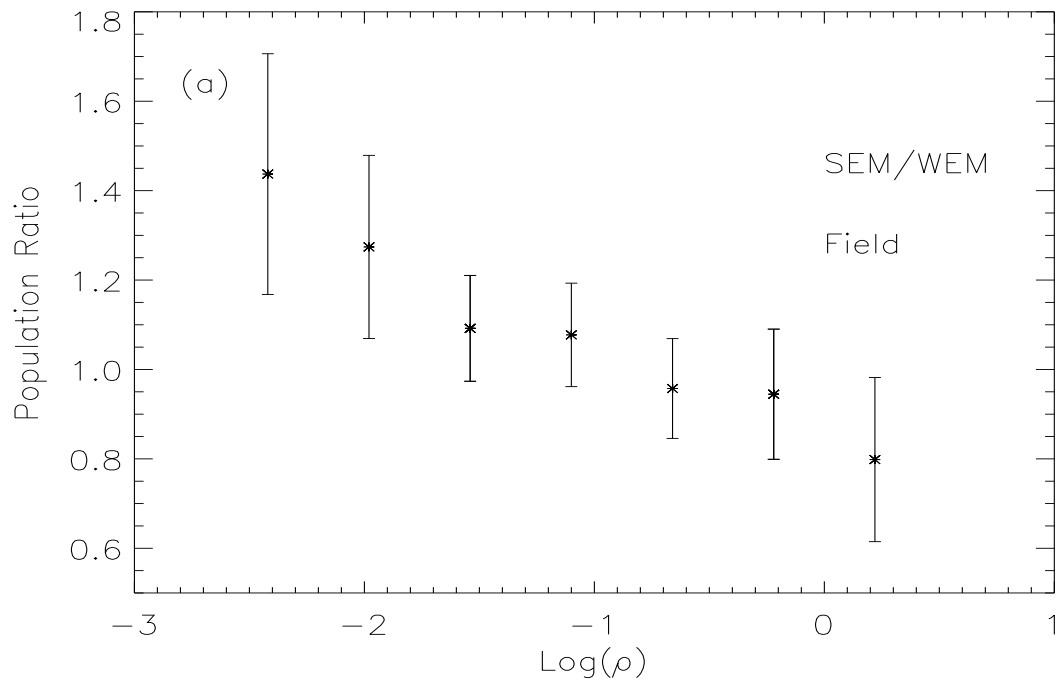


Fig. 6

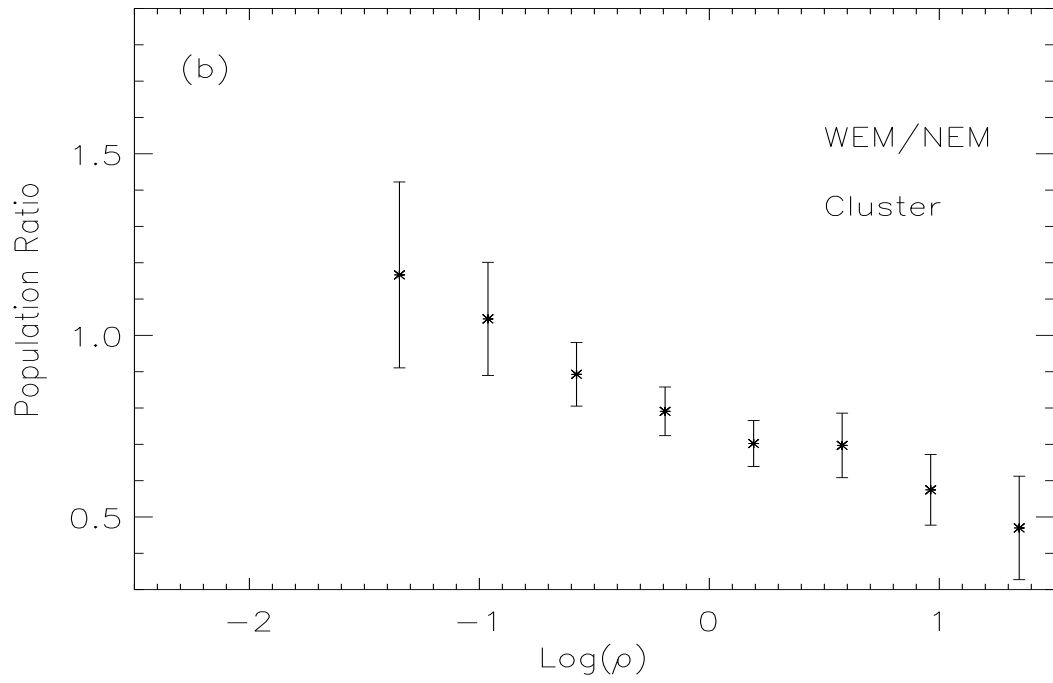
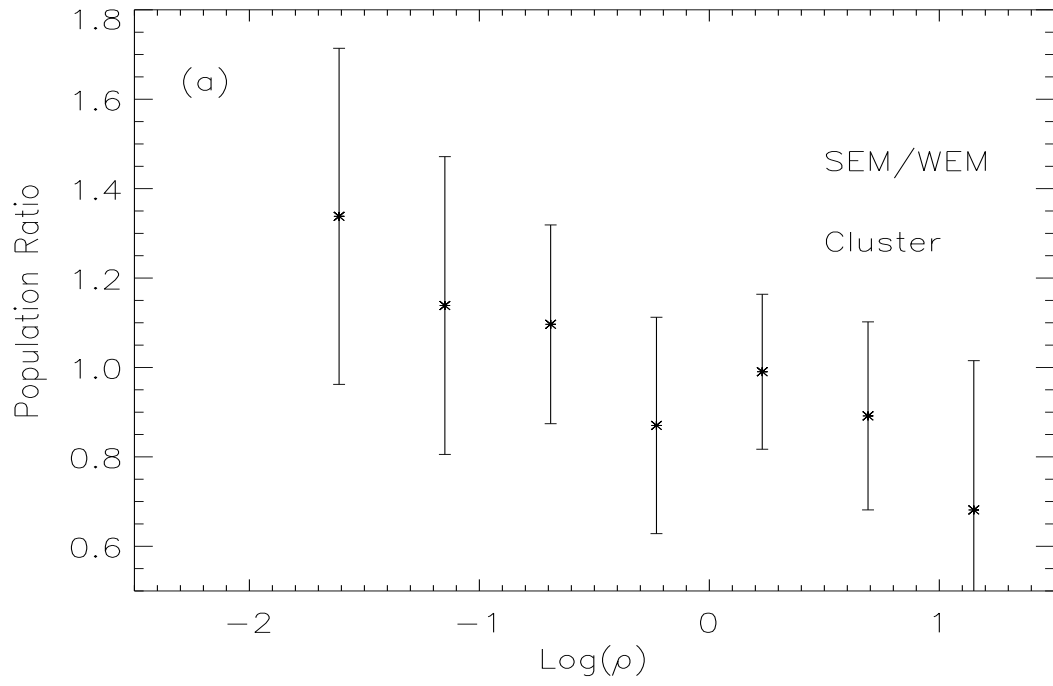


Fig. 7

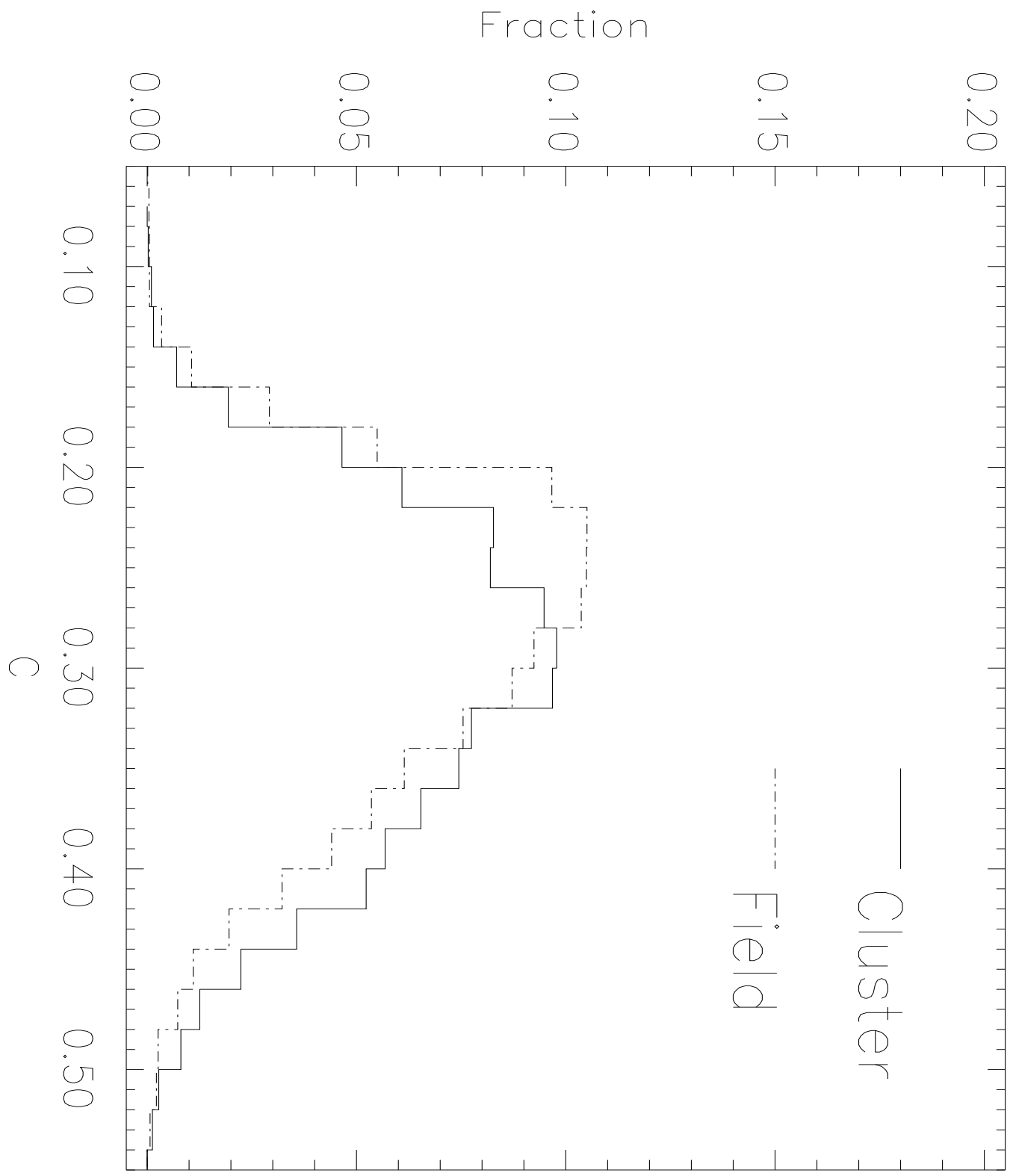


Fig. 8

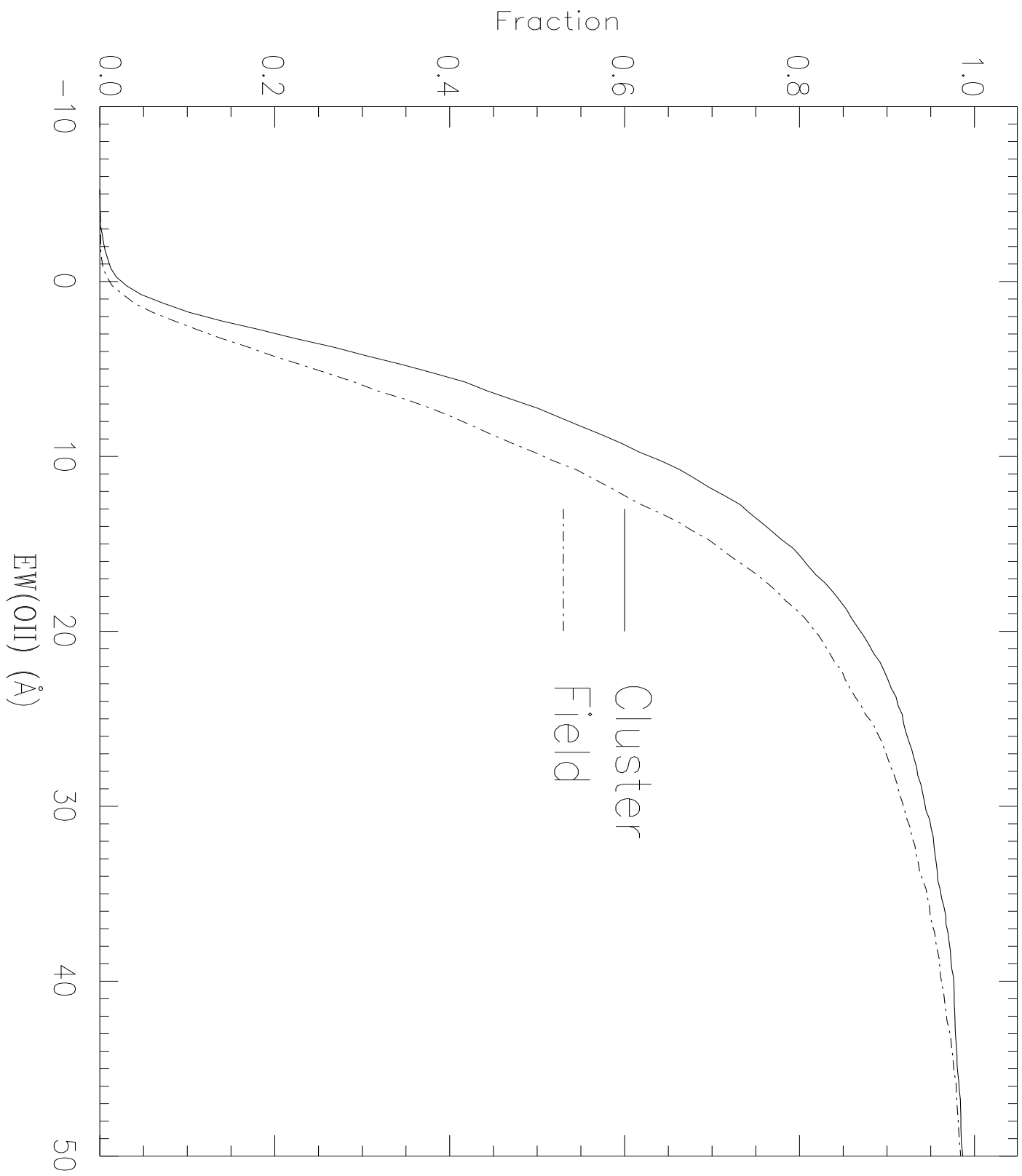


Fig. 9

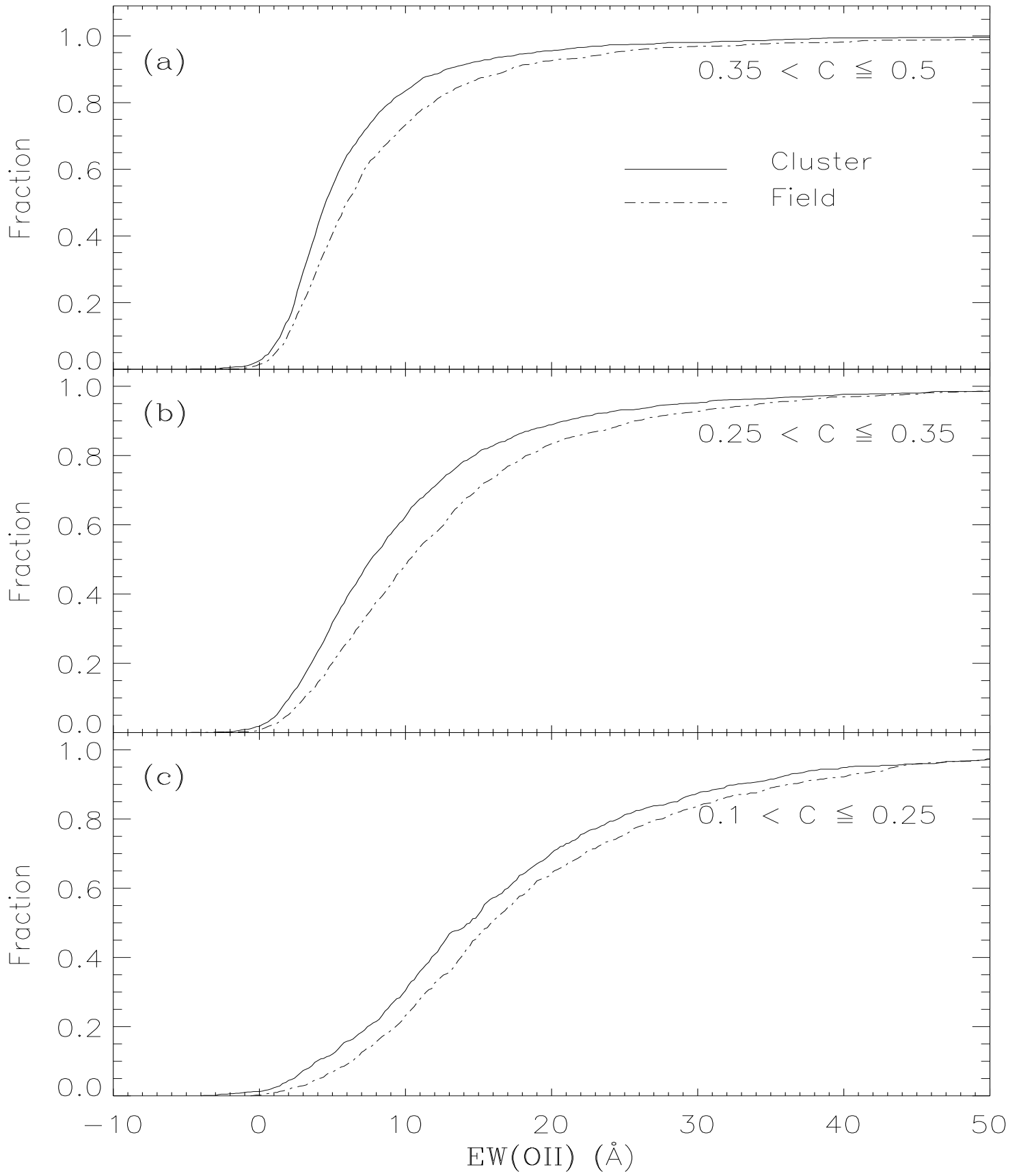


Fig. 10